

# Fabrication of GaAs, $\text{In}_x\text{Ga}_{1-x}\text{As}$ and Their ZnSe Core/Shell Colloidal Quantum Dots

Joong Pill Park,<sup>†</sup> Jae-joon Lee,<sup>‡</sup> and Sang-Wook Kim<sup>\*,†</sup>

<sup>†</sup>Department of Molecular Science and Technology, Ajou University, Suwon 443-749, Korea

<sup>‡</sup>Department of Energy & Materials Engineering, Dongguk University Seoul 100-715, Korea

**S** Supporting Information

**ABSTRACT:** We first report the GaAs/ZnSe and  $\text{In}_x\text{Ga}_{1-x}\text{As}/\text{ZnSe}$  core/shell structured colloidal quantum dots (CQDs). GaAs based CQD, which are hard to obtain by the chemical synthetic method, can be prepared successfully using the acetylacetonate complex of indium and gallium as cationic precursors. We control the indium contents, and the photoluminescence emission is tuned from orange to deep red.  $\text{In}_{0.2}\text{Ga}_{0.8}\text{As}/\text{ZnSe}$  core/shell QDs show the best quantum yield of 25.6%. A ZnSe outer shell protects the core and improves quantum yield, and it shows a large red shift owing to the quasi-type-I band structure.

It is well-known GaAs is an important semiconductor material that has attracted significant attention because of its use in solar cells and optoelectronics. It has a direct bandgap of 1.42 eV and a zinc blende crystal structure.<sup>1,2</sup> Similar to other semiconductor materials, GaAs shows quantum confinement effects as the particle size decreases below the Bohr exciton radius of about 10 nm<sup>3,4</sup> (they are then called quantum dots, QDs), leading to visible light absorption and emission. To date, GaAs QDs have been generally fabricated by physical methods such as molecular beam epitaxy (MBE)<sup>5–7</sup> and metalorganic chemical vapor deposition (MOCVD).<sup>8–10</sup> In MOCVD, highly reactive alkyl metal precursors can be used to control alloy composition and realize various shapes, including dots, wires,<sup>11</sup> and wells.<sup>12,13</sup> However, this method has found limited use in film formation. Various fields of applications need good processable QD states, especially colloidal QDs (CQDs); therefore, chemical synthesis methods have been recommended. Recently, the synthesis of GaAs CQDs via a general CQD synthetic method has been reported; the synthesis involves a high-temperature reaction of precursors in a coordinating solvent and surfactant. GaAs CQDs have been studied since the early 90s, but they have poor properties preventing further applications. Olshavsky et al. first reported colloidal GaAs CQDs based on a quinoline coordinating solvent.<sup>14</sup> Uchida et al. and Salata et al. used polar media for the synthesis of uniform-sized particles such as poly(vinyl alcohol) (PVA) and triethylene glycol dimethyl ether.<sup>15,16</sup> Some groups have been trying to synthesize nanosized GaAs particles via homogeneous vapor-phase nucleation or a thermal evaporation method.<sup>17,18</sup> However, good-quality QDs with high quantum yield (QY) and well-tuned bandgap have not been obtained.

III-V CQDs, including GaAs CQDs, have more covalent and oxidative characteristics than II-VI CQDs; therefore, their surface passivation is very important. Usually, another inorganic shell material that has the same crystalline structure, similar lattice parameters, and a wide bandgap is used, for example, zinc sulfide (ZnS) and zinc selenide (ZnSe). The core/shell structures lead to high QY, improved emission peak width, and a slightly red-shifted emission. Among the III-V CQDs, most studies have focused on indium phosphide (InP) and their core/shell structures, including InP/ZnS, InP/ZnSe, and InP/GaP/ZnS, because they are cadmium free, emit visible light, and have a high QY and a narrow emission peak width, which can be used in commercial displays. However, core/shell structures of other III-V CQDs, including GaP<sup>19,20</sup> and GaAs<sup>14–18</sup> CQDs have been rarely studied. Formation of II-VI outer shells such as from ZnS and ZnSe is difficult on III-V CQDs compared to that on II-VI CQD cores owing to the problem of charge balance. To form the II-VI outer shell, intermediate layers are inserted for reducing the lattice mismatch and charge difference.<sup>21,22</sup> Herein, we present well-controlled GaAs and InGaAs CQDs. Their photoluminescence (PL) emission was tuned in the visible range by controlling the amount of indium. ZnSe was selected as the outer shell material because it has a similar lattice parameter. After forming a ZnSe outer shell, the QY improved dramatically, similar to other QDs.<sup>23,24</sup> Finally, the emission wavelength could be tuned from 580 to 700 nm, and  $\text{In}_{0.2}\text{Ga}_{0.8}\text{As}/\text{ZnSe}$  showed the best QY of 25.6%. In our experiments, the acetylacetonate forms of indium and gallium were used as cationic precursors for leading the reaction. To know the information on real precursors or intermediates, the sample after degassing process was analyzed using FAB-mass technique (Supporting Information S3). The data shows that only one acetylacetonates group was exchanged and changed to dimer and trimer type of Ga. As a result, the acetylacetonates are still attached to Ga after degassing process and influence on QD synthetic process. The binding energy of acetylacetonate ligand to metal cation is very weak compared to that of other common ligands including acetate and halide. Halide is a strong X-type ligand and acetate is an L-type ligand, but it has a slightly stronger binding energy.<sup>25</sup> We have used a modified form of our previous heating procedure for InP based core/shell/shell QDs.<sup>26</sup> GaAs CQD was synthesized using gallium(III) acetylacetonate ( $\text{Ga}(\text{acac})_3$ ) and tris-(trimethylsilyl) arsenide ( $\text{TMS}_3\text{As}$ ) as precursors. When the

Received: August 19, 2016

Published: December 15, 2016

TMS<sub>3</sub>As was added to the colorless and transparent Ga(acac)<sub>3</sub> precursor solution of octadecene, the solution became light red, indicating the formation of a Ga–As complex, which is similar to the formation of In–P complex.

The red color changed to dark red as the reaction temperature was elevated to 300 °C. The final product was obtained using the usual purification process,<sup>26</sup> and analyzed using X-ray diffraction (XRD), transmission electron microscopy (TEM), and scanning transmission electron microscopy (STEM). The diameters of GaAs and GaAs/ZnSe QDs were determined to be 1.8 and 3 nm, respectively (Figure 1c,d).

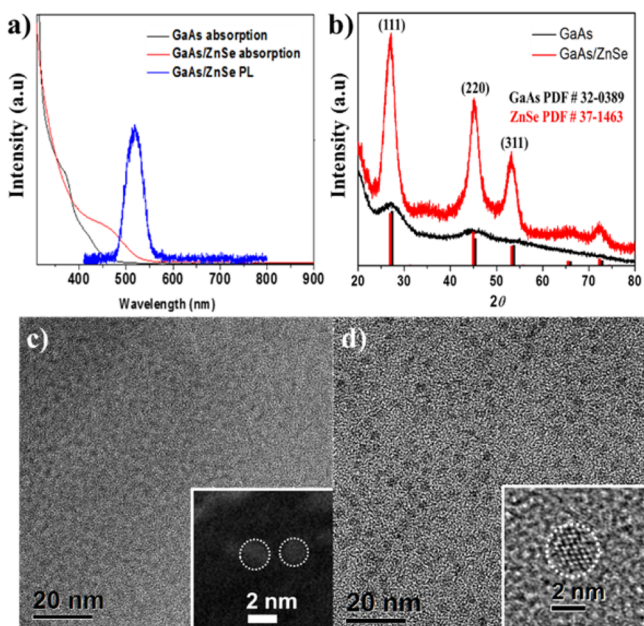


**Figure 1.** (a) Absorption and photoluminescence (PL) spectrum of GaAs and GaAs/ZnSe; GaAs only has absorption spectra, and GaAs/ZnSe has weak PL. (b) PXRD data of GaAs and GaAs/ZnSe. (c) TEM image and STEM image (inset ~1.5 nm) of GaAs core. (d) TEM image of GaAs/ZnSe, and their HR-TEM image (inset ~3 nm).

They were roughly spherical in shape. Powder XRD (PXRD) patterns indicated that the GaAs and GaAs/ZnSe QDs have the same zinc blende structures (Figure 1b), which were indexed to the (111), (220), and (311) planes. The broad peak pattern resulted from the small crystal size and poor crystallinity. The GaAs core showed a distinct optical absorption edge; however, no PL emission was observed. Generally, the numerous surface traps of GaAs III–V QDs have been known to cause poor optical properties,<sup>29,30</sup> and a core/shell structure has been suggested to improve the optical properties. In this work, ZnSe was selected for the formation of the outer shell. GaAs and ZnSe have the same zinc blende crystal structure and very similar lattice parameters of 0.565 and 0.566 nm, respectively. Therefore, a ZnSe shell can be formed easily on GaAs CQDs without interfacial strain. Successful shell formation was confirmed by PXRD and TEM measurement. The diffraction patterns are not shifted, but peak intensities are increased because of similar lattice parameters and high crystallinity. The particle size is also increased and highly crystalline images are observed (Figure 1d inset). In the band offsets, the GaAs/ZnSe core/shells have typical type-I structures. Therefore, surface passivation, and as a result, QY improvement and a little red-shift in the absorption can be expected. In Figure 1a, the first

excitonic absorption peak is shifted toward the long wavelength region. The QY improvement was not significant though shell formation, and a weak PL emission in the GaAs/ZnSe was observed (QY < 1%).

To improve the optical properties of GaAs QDs, including QY and emission color tuning, an indium alloy system was introduced. Until now, an In<sub>x</sub>Ga<sub>1-x</sub>As alloy system has been usually fabricated by the physical method for bandgap tuning, and used for optoelectronic applications in the NIR region.<sup>27,28</sup> Here, In<sub>x</sub>Ga<sub>1-x</sub>As and their ZnSe core/shell CQD structure were developed using the chemical synthesis method. Various compositions of In<sub>x</sub>Ga<sub>1-x</sub>As QD alloys were fabricated using a synthesis method similar to that for GaAs QDs, with the exception being that an indium precursor was used. The detailed procedures are shown in the Supporting Information. The possibility of formation of a core/shell structure, for example, InAs/GaAs or GaAs/InAs was ruled out as InAs/GaAs should exhibit PL with a longer wavelength because of the InAs bandgap and type-I band offsets. The synthesis of InAs that emits green light is difficult. The possibility of GaAs/InAs was excluded because of the relative reactivity between the In–As and Ga–As complex. Elemental analysis using inductively coupled plasma-atomic emission spectroscopy (ICP-AES) was used to determine that indium to gallium precursor ratios of 10/90, 20/80, and 30/70 produced QDs with indium to gallium ratios of 10/70, 25/75, and 38/62, respectively (see Supporting Information). This is because of the ease of formation of the In–As complex compared to the Ga–As complex. We controlled the precursor ratio of indium to gallium and obtained five samples with an indium to gallium ratio of 1:9, 2:8, 3:7, 5:5, and 7.5:2.5. PXRD analysis showed three peaks, which were indexed to the (110), (211), and (310) planes of a cubic zinc blende structure at all compositions. The diffraction patterns transformed from those for GaAs to those corresponding to InAs as the indium content increased, but in the case of the 5:5 and 7.5:2.5 compositions, the peaks almost corresponded to InAs (Figure S1). The PL emission wavelengths of In<sub>x</sub>Ga<sub>1-x</sub>As and In<sub>x</sub>Ga<sub>1-x</sub>As/ZnSe were red-shifted when the indium content increased. The emissions of In<sub>x</sub>Ga<sub>1-x</sub>As could be tuned from green to orange, but they showed poor stability and disappeared soon. Their core/shell structures showed improved optical properties and could be tuned from orange to a deep red color (Figure 2b–d). Interestingly, the emission wavelength showed a large shift of over 50 nm when the ZnSe shell was coated. Finally, the PL emission could be tuned between 570 and 690 nm by controlling the indium content (5%–30%). Among them, In<sub>0.2</sub>Ga<sub>0.8</sub>As/ZnSe showed the best QY of 25.6%. As mentioned above, the bandgap of the In<sub>1-x</sub>Ga<sub>x</sub>As core was tuned in the visible range, and the core was coated with ZnSe, which is a well-known wide bandgap material. Therefore, the band structure of InGaAs/ZnSe was considered to be type-I. Though the CQDs have a type-I bandgap structure, the electron present in the core can be found in the shell because of tunneling.<sup>31</sup> Therefore, the PL emission is slightly red-shifted. In our experiment, a large shift in emission occurred. In the case of In<sub>0.2</sub>Ga<sub>0.8</sub>As, the absorption peak moved from 500 to 600 nm (Figure 2e). A large shift is usually observed in a type-II band structure.

To confirm the band structure, the core and core/shell structure of In<sub>0.2</sub>Ga<sub>0.8</sub>As were analyzed using cyclic voltammetry (CV). The measurement was carried out with film type, and scan rate was 1 mV/s. Ag/AgCl reference electrode, a Pt



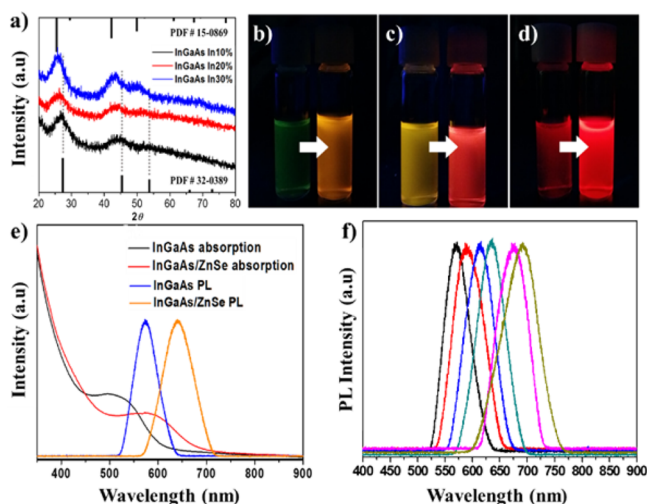


**Figure 2.** (a) XRD data of  $\text{In}_x\text{Ga}_{1-x}\text{As}$  of various indium contents. (b–d) Photographs of  $\text{In}_x\text{Ga}_{1-x}\text{As}$  (left) and ZnSe shell QDs (right); the contents of added-indium was controlled 10% (b), 20% (c), and 30% (d). (e) Normalized PL and absorption spectrum of  $\text{In}_{0.2}\text{Ga}_{0.8}\text{As}$  and their ZnSe shell QDs. (f) Normalized PL spectrum of various  $\text{In}_{1-x}\text{Ga}_x\text{As}/\text{ZnSe}$  QDs; indium contents 5%–30%.

counter electrode and glassy carbon working electrode were used. Lithium perchlorate acetonitrile solution of 0.1 M was used as the electrolyte. The thin layer of QD was formed on the glassy carbon electrode. A drop of diluted QD–hexane solution was drop-casted and dried, and it was repeated three times. The CV curve showed multiple  $\text{offset}_{\text{red}}$  and  $\text{offset}_{\text{ox}}$  values (Figure 3b). The band offset calculated using the absorption peak

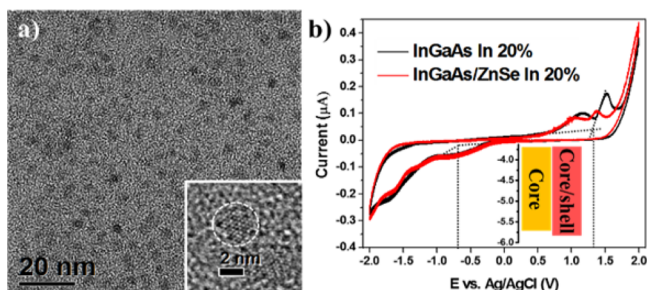


**Figure 3.** Core and core–shell structure was analyzed for band structure study. The TEM image of  $\text{In}_{0.2}\text{Ga}_{0.8}\text{As}/\text{ZnSe}$  (inset: HR image) (a), and CV data and band diagram (inset) (b).

(Figure 2e) is 2.032 eV, and the best matching result is 1.996 eV from an  $\text{offset}_{\text{red}}$  of  $-0.686$  V and an  $\text{offset}_{\text{ox}}$  of 1.31 V. Compared to the CV curve of the core/shell structure, the oxidation peaks are different by 0.13 eV, but the reduction peaks are almost the same. The oxidation and reduction corresponded to the HOMO and LUMO levels.<sup>32–34</sup> Therefore, the  $\text{In}_{0.2}\text{Ga}_{0.8}\text{As}$  core and ZnSe shell have similar LUMO levels, and the band structure can be classified as a quasi-type-I structure. This results seem to be concerned with similar LUMO levels of bulk GaAs and ZnSe.<sup>35</sup> As a result, the large shift in the emission from the core/shell structure can be explained.

In summary, we have synthesized GaAs and GaAs/ZnSe CQDs using a metal acetylacetonate precursor and a common fatty acid–ODE system. Their optical properties are not satisfactory, therefore, we introduced the  $\text{In}_x\text{Ga}_{1-x}\text{As}$  alloy

system for improving them. The  $\text{In}_x\text{Ga}_{1-x}\text{As}$  alloy system show better optical properties, and its PL wavelength was controlled by the indium content. A ZnSe outer shell protects the core and improves QY, and it shows a large red shift owing to the quasi-type-I band structure. These results indicate the potential of possible NIR optoelectronic materials and can encourage further research on novel material synthesis

## ■ ASSOCIATED CONTENT

### Supporting Information

The Supporting Information is available free of charge on the ACS Publications website at DOI: 10.1021/jacs.6b08679.

PXRD, FAB-mass, ICP data, synthetic procedure (PDF)

## ■ AUTHOR INFORMATION

### Corresponding Author

\*swkim@ajou.ac.kr

### ORCID

Sang-Wook Kim: 0000-0001-6301-6550

### Notes

The authors declare no competing financial interest.

## ■ ACKNOWLEDGMENTS

This work was supported by the Basic Science Research Program (No. 2014R1A5A1009799), the Priority Research Program (2009-0093826) and C1 Gas Refinery Program (2015M3D3A1A 01064899) funded by the Ministry of Science, ICT & Future Planning, and by the New & Renewable Energy Core Technology Program (No. 20133030000140) of KETEP granted financial resource from the Ministry of Trade, Industry & Energy, Republic of Korea.

## ■ REFERENCES

- Hiruma, K.; Yazawa, M.; Haraguchi, K.; Ogawa, K.; Katsuyama, T.; Koguchi, M.; Kakibayashi, H. *J. Appl. Phys.* **1993**, *74*, 3162.
- Zhang, X.-C.; Jin, Y.; Ware, K.; Ma, X. F.; Rice, A.; Bliss, D.; Larkin, J.; Alexander, M. *Appl. Phys. Lett.* **1994**, *64*, 622.
- Peter, A. J.; Navaneethakrishnan, K. *Phys. E* **2008**, *40*, 2747.
- Shi, W. S.; Zheng, Y. F.; Wang, N.; Lee, C. S.; Lee, S. T. *Appl. Phys. Lett.* **2001**, *78*, 3304.
- Stievater, T. H.; Li, X.; Steel, D. G.; Gammon, D.; Katzer, D. S.; Park, D.; Piermarocchi, C.; Sham, L. J. *Phys. Rev. Lett.* **2001**, *87*, 133603.
- Matsuda, K.; Saiki, T.; Nomura, S.; Mihara, M.; Aoyagi, Y.; Nair, S.; Takahara, T. *Phys. Rev. Lett.* **2003**, *91*, 177401.
- Rastelli, A.; Stuffer, S.; Schliwa, A.; Songmuang, R.; Manzano, C.; Costantini, G.; Kern, K.; Zrenner, A.; Bimberg, D.; Schmidt, O. G. *Phys. Rev. Lett.* **2004**, *92*, 166104.
- Arakawa, Y.; Nagamune, Y.; Nishioka, M.; Tsukamoto, S. *Semicond. Sci. Technol.* **1993**, *8*, 1082.
- Li, R. R.; Dapkus, P. D.; Thompson, M. E.; Jeong, W. G.; Harrison, C.; Chaikin, P. M.; Register, R. A.; Adamson, D. H. *Appl. Phys. Lett.* **2000**, *76*, 1689.
- Park, J. H.; Khandekar, A. A.; Park, S. M.; Mawst, L. J.; Kuech, T. F.; Nealey, P. F. *J. Cryst. Growth* **2006**, *297*, 283.
- Tsukamoto, S.; Nagamune, Y.; Nishioka, M.; Arakawa, Y. *J. Appl. Phys.* **1992**, *71*, 533.
- Levine, B. F.; Bethea, C. G.; Glogovsky, K. G.; Stayt, J. W.; Leibenguth, R. E. *Semicond. Sci. Technol.* **1991**, *6*, C114.
- Tansu, N.; Mawst, L. J. *IEEE Photonics Technol. Lett.* **2001**, *13*, 179.
- Olshavsky, M. A.; Goldstein, A. N.; Alivisatos, A. P. *J. Am. Chem. Soc.* **1990**, *112*, 9438.

- (15) Salata, O. V.; Dobson, P. J.; Hull, P. J.; Hutchison, J. L. *Appl. Phys. Lett.* **1994**, *65*, 189.
- (16) Uchida, H.; Curtis, C. J.; Kamat, H. V.; Jones, K. M.; Nozik, A. J. *J. Phys. Chem.* **1992**, *96*, 1156.
- (17) Sercel, P. C.; Saunders, W. A.; Atwater, H. A.; Vahala, K. J.; Flagan, R. C. *Appl. Phys. Lett.* **1992**, *61*, 696.
- (18) Hung, J.; Lee, S.-C.; Chia, C.-T. *J. Nanopart. Res.* **2004**, *6*, 415.
- (19) Manciu, F. S.; Sahoo, Y.; MacRae, D. J.; Furis, M.; McCombe, B. D.; Prasad, P. N. *Appl. Phys. Lett.* **2003**, *82*, 4059.
- (20) Kim, Y.-H.; Jun, T.-w.; Jun, B.-H.; Lee, S.-M.; Cheon, J. *Am. Chem. Soc.* **2002**, *124*, 13656.
- (21) Virieux, H.; Le Troedec, M.; Cros-Gagneux, A.; Ojo, W.; Delpech, F.; Nayral, C.; Martinez, H.; Chaudret, B. *J. Am. Chem. Soc.* **2012**, *134*, 19701.
- (22) Pietra, F.; De Trizio, L.; Hoekstra, A. W.; Renaud, N.; Prato, M.; Grozema, F. C.; Baesjou, P. J.; Koole, R.; Manna, L.; Houtepen, A. J. *ACS Nano* **2016**, *10*, 4754.
- (23) Cao, Y. W.; Banin, U. *J. Am. Chem. Soc.* **2000**, *122*, 9692.
- (24) Millo, O.; Katz, D.; Cao, Y. W.; Banin, U. *Phys. Status Solidi B* **2001**, *224*, 271.
- (25) Skinner, H. A.; Connor, J. A. *Pure Appl. Chem.* **1985**, *57*, 79.
- (26) Park, J. P.; Lee, J.-J.; Kim, S.-W. *Sci. Rep.* **2016**, *6*, 30094.
- (27) Sellin, R. L.; Ribbat, Ch.; Grundmann, M.; Ledentsov, N. N.; Bimberg, D. *Appl. Phys. Lett.* **2001**, *78*, 1207.
- (28) Kim, S. M.; Wang, Y.; Keever, M.; Harris, J. S. *IEEE Photonics Technol. Lett.* **2004**, *16*, 377.
- (29) Deppe, D. G.; Holonyak, N., Jr. *J. Appl. Phys.* **1988**, *64*, R93.
- (30) del Alamo, J. A. *Nature* **2011**, *479*, 317.
- (31) Reiss, P.; Protière, M.; Li, L. *Small* **2009**, *5*, 154.
- (32) Haram, S. K.; Quinn, B. M.; Bard, A. J. *J. Am. Chem. Soc.* **2001**, *123*, 8860.
- (33) Inamdar, S. N.; Ingole, P. P.; Haram, S. K. *ChemPhysChem* **2008**, *9*, 2574.
- (34) Hyun, B.-R.; Zhong, Y.-W.; Bartnik, A. C.; Sun, L.; Abruña, H. D.; Wise, F. W.; Goodreau, J. D.; Matthews, J. R.; Leslie, T. M.; Borrelli, N. F. *ACS Nano* **2008**, *2*, 2206.
- (35) Norris, D. J.; Efros, A. L.; Erwin, S. C. *Science* **2008**, *319*, 1776.